Effect of Phosphorylation on α-Helix Stability as a Function of Position†

Charles D. Andrew,‡ Jim Warwicker,‡ Gareth R. Jones,§ and Andrew J. Doig*,‡

Department of Biomolecular Sciences, UMIST, P.O. Box 88, Manchester M60 1QD, U.K., and Daresbury Laboratory, Daresbury, Warrington, Cheshire WA4 4AD, U.K.

Received June 25, 2001; Revised Manuscript Received November 5, 2001

ABSTRACT: We have investigated the effect of placing phosphoserine at the N-cap, N1, N2, N3, and interior position in alanine-based α-helical peptides. Helix contents of each peptide were measured by CD spectroscopy and titrations performed to determine pK_a values. Data were analyzed with modified Lifson−Roig theory to determine helix-coil parameters (n, n_1, n_2, n_3, and w) and free energy changes for phosphoserine at each helical position. Results are given for a −1 and −2 phosphoserine charge state. Results show that phosphoserine stabilizes at the N-terminal positions by as much as 2.3 kcal·mol^{-1}, while destabilizes in the helix interior by 1.2 kcal·mol^{-1}, relative to serine. The rank order of free energies relative to serine at each position is N2 > N3 > N1 > N-cap > interior. Moreover, −2 phosphoserine is the most preferred residue known at each of these N-terminal positions. Experimental pK_a values for the −1 to −2 phosphoserine transition are in the order N2 < N-cap < N1 < N3 < interior. This order agrees well with electrostatics calculations carried out with phosphoserine at the N-terminal positions and interior positions. Combining these with calculations at the C3, C2, C1, and C-cap positions gives results for phosphoserine along the length of the helix. We see a transition from phosphoserine stabilization at the N-terminus to destabilization at the C-terminus and can explain this in terms of the balance of protein solvation, favorable interactions, and dehydration. These results give insight into the phosphorylatable control of biological systems through positive or negative changes in stability.

The reversible phosphorylation of amino acids is a widespread control mechanism in biochemical processes (*1*). Protein phosphorylation is ubiquitous, yet how this modification affects proteins is poorly understood in structural and energetic terms. Here we make a detailed study of the effects of phosphorylating serine side chains within an α-helix, showing that the effects vary greatly at different positions within the helix and can give very strong interactions, greater than for any of the standard 20 amino acids. This suggests general mechanisms by which phosphorylation modulates protein structure and function.

Davies (1964) first showed that some amino acid residues occur more than others in the helix, as noted later by others (*2*−*4*). More detailed examination of amino acid preferences in the α-helix revealed a greater complexity, because the frequency of an amino acid depends on its position in the helix. Residues following the N-cap have helical ϕ, ψ angles and are labeled N1, N2, N3, N4, etc. Studies revealed that the helix has significantly different residue frequencies for the N-cap, N1, N2, N3 and helix interior positions (*5*−*7*). The N-cap residue immediately precedes the helix N-terminus and has nonhelical ϕ, ψ angles, but its carbonyl group participates in the first backbone helical hydrogen bond. The amide NH groups of N-cap, N1, N2, and N3 do not take part in i, $i + 4$ backbone hydrogen bonds that characterize the α-helix. The presence of these otherwise unsatisfied hydrogen-bond donors has profound structural effects, most often satisfied by hydrogen bonds to side chains local in sequence, such as to preceding N-cap side chains.

The N-cap residue is now well-understood in terms of its effect on the stability and structure of the α-helix. Experimental measurement of N-caps in peptides (*8*−*13*) and proteins (*14*−*17*) revealed that Ser, Thr, Asn, and Asp$^-$ have high preferences for this position, as their side chains adopt favorable rotamer conformations to hydrogen bond to free backbone NH groups. Our recent studies of the N1, N2, and N3 positions in proteins highlighted strong structural preferences unique to these positions at the N-terminus (*18*). Experiments in peptides show similar preferences to these structural studies but negative residues Asp$^-$ and Glu$^-$ are preferred at N1 and N2 over neutral good hydrogen bond formers such as Ser and Asn (*19*−*23*). These preferred amino acids were rationalized by favorable electrostatic interactions with the helix dipole, as side chains at N1 and N2 have poor geometry for hydrogen bonding, unlike the linear hydrogen bonds associated with good N-cap residues. Helix termini are highly solvent exposed and tertiary interactions are rare, so the environment of peptide and protein helices are very similar.

It has been shown that phosphoserine stabilizes at N-terminal helical positions in proteins (*24*) and in simulations (*25*) while it destabilizes at the interior (*26*), although free energies have not been measured for all these positions. Here we carry out an extensive study of the effect of phosphoserine

† C.D.A. is the grateful recipient of a BBSRC (UK) studentship with CASE award (Daresbury). We thank the Wellcome trust for an equipment grant for the CD spectrometer (ref 057318).

* To whom correspondence should be addressed. Telephone: +44-161-200-4224. Fax: +44-161-236-0409. E-mail: Andrew.Doig@umist.ac.uk.

‡ UMIST.

§ Daresbury Laboratory.

10.1021/bi0113216 CCC: $22.00
Published on Web 01/16/2002

Table 1: Sequences and Helix Contents of Peptides

name	sequence	$[\theta]_{222}$[a] Ser	% helicity[b]	$[\theta]_{222}$[a] (P)Ser −1	% helicity[b]	$[\theta]_{222}$[a] (P)Ser −2	% helicity[b]
Ser N-cap	SAAAAQRAAAARAGY-NH_2	−9800[c]	30.5				
Ser(P) N-cap	S(P)AAAAQRAAAARAGY-NH_2			−5200	17.1/23.7[d]	−15500	47.3
Ser N1	Ac-SAAAAQRAAAARAGY-NH_2	−16500	49.5				
Ser(P) N1	Ac-S(P)AAAAQRAAAARAGY-NH_2			−17000	50.8	−20400	60.6
Ser N2	Ac-ASAAAAQRAAAARGY-NH_2	−14100	42.4				
Ser(P) N2	Ac-AS(P)AAAAQRAAAARGY-NH_2			−18900	56.3	−22800	67.7
Ser N3	Ac-AASAAAAQRAAAARGY-NH_2	−14100	42.0				
Ser(P) N3	Ac-AAS(P)AAAAQRAAAARGY-NH_2			−16500	48.8	−18400	54.1
Ser mid	Ac-AAAQRAAAASAAAARGY-NH_2	−12900	38.0				
Ser(P) mid	Ac-AAAQRAAAAS(P)AAAARGY-NH_2			−8300	25.2	−5500	17.2

[a] Mean residual ellipticities measured in deg cm^2 $dmol^{-1}$ at 222 nm. [b] Calculated as $[\theta]_{222}$(observed) − $[\theta]_{222}$(coil)/[−42500(1 − 3/*n*) − $[\theta]_{222}$(coil)], where $[\theta]_{222}$ (coil) is 640 deg cm^2 $dmol^{-1}$ and *n* is the number of amino acids in the peptide (*29*). [c] Neutral N-terminus. [d] Corrected value for −1 phosphoserine with neutral N-terminus, using average free energy for protonation of N-terminus (0.83 kcal mol^{-1}), from Doig and Baldwin (*13*).

in helical peptides, giving free energies for a range of positions.

PEPTIDE DESIGN

Peptides are based on the control sequence Ac-SAAA-AQRAAAARAGY-NH_2, utilizing the high helix propensity of alanine. Alanine-based sequences, solubilized by appropriately spaced polar side chains, are monomeric in aqueous solution (*27*). Sequences are designed to avoid all *i*, *i* + 3, and *i*, *i* + 4 interactions between other side chains. Gly is a helix breaker and is placed between tyrosine and the rest of the sequence to prevent unwanted interaction between the aromatic chromophore and the rest of the helix, which may contribute to the CD[1] signal (*28*). Tyrosine is positioned at the C-terminus to allow concentration determination. Glutamine and arginine are present for solubility.

The N- and C-termini are blocked with an acetyl and amide group, respectively, which prevent destabilizing interactions with these charged termini and the helix dipole. The acetyl group is therefore the N-cap and the amide group the C-cap, if the peptide is completely helical. This also decreases the number of free main chain amine and carboxyl groups, by creating an extra hydrogen bond at each terminus. Acetyl groups also stabilize the helix (*12*). The acetyl group is removed and replaced by phosphoserine at the N-cap position when determining N-cap preferences (*n* values). Phosphoserine is positioned in acetylated peptides at N1, N2, and N3 and in the helix interior (see sequences in Table 1), allowing determination of N1, N2, and N3 and interior preferences (n_1, n_2, n_3, and *w* values, respectively).

Peptides are designed to be approximately 50% helical, where ellipticity is most sensitive to small changes in interaction energy, using helix/coil theory to predict helix contents. Helix content is measured by the molar residual ellipticity at 222 nm. Modified Lifson−Roig theory (*21, 29*) is fitted to the experimental data, allowing free energies for the phosphoserine residue to be calculated for each position. We did not synthesize peptides with phosphoserine at C-terminal positions, because phosphorylation is expected to be highly destabilizing at these positions (supported by electrostatics calculations, below). The helix content in the region of the phosphorylation site will be close to zero, precluding determining an accurate value for the energetic effects of phosphorylation on helix stability.

MATERIALS AND METHODS

Peptide Synthesis. Peptides were synthesized on an Applied Biosystems 431A peptide synthesizer using Fmoc solid-phase chemistry. 9-Fluoroenylmethoxycarbonyl amino acids (CN Biosciences) were coupled to rink amide resin (CN Biosciences) using 2(1*H*-benzotriazol-1-yl)-1,1,3,3-tetramethyluronium tetrafluoroborate (TBTU) and *N*-hydroxybenzotriazole·H_2O (HOBt) with an *N*,*N*-diisopropylethylamine (NMP) solvent. Acetylation of N-termini was carried out with pyridine and acetic anhydride. Cleavage from the resin and removal of Ser, Ser(P), Gln, Arg, and Tyr side chain protecting groups was accomplished with 95% trifluoroacetic acid, 2.5% triisopropylsilane, and 2.5% H_2O.

Peptides were purified using C_{18} reverse-phase HPLC (Hewlett-Packard Series 1100) using 5−40% H_2O/acetonitrile gradients in the presence of 0.1% trifluoroacetic acid. Peptide verification was achieved by Electrospray mass spectrometry at the Michael Barber Centre for Mass Spectrometry, UMIST, Manchester, U.K.

Circular Dichroism Measurements. CD measurements were made using a Jasco J810 spectropolarimeter. The buffer used for pH titrations contained 10 mM NaCl, 1 mM sodium phosphate, 1 mM sodium borate, and 1 mM sodium citrate. Measurements were taken at 273 K, pH 7.0, in a 1.0 cm quartz cell. The pH was adjusted during the titrations with aliquots of 1 M HCl and 1 M NaOH. The ellipticity data from these titrations were fitted to a Henderson−Hasselbach equation to determine the pK_a values. An equation for three pK_a values

$$[\theta]_{222nm} = [\theta]_{222,mid\_pH}\left(1 - \frac{1}{1 + 10^{pH-pK_{a1}}}\right) + [\theta]_{222,low\_pH}\left(\frac{1}{1 + 10^{pH-pK_{a1}}}\right) + [\theta]_{222,(mid\_pH-high\_pH)}\left(1 - \frac{1}{1 + 10^{pH-pK_{a2}}}\right)$$

was used for analyzing the unacetylated Ser(P) N-cap, while an equation for two pK_a values

[1] Abbreviations: cAMP, cyclic adenine monophosphate; CD, circular dichroism; FDPB, finite difference Poisson−Boltzmann; HOBt, *N*-hydroxybenzotriazole·H_2O; HPLC, high-pressure liquid chromatography; HPr, histidine containing protein; KID, kinase-inducible domain; KIX, KIX domain; NMP, *N*,*N*-diisopropylethylamine; TBTU, tetramethyluronium tetrafluoroborate.

$$[\theta]_{222nm} = [\theta]_{222,mid^1\_pH}\left(1 - \frac{1}{1 + 10^{pH-pK_{a1}}}\right) + [\theta]_{222,low\_pH}*\left(\frac{1}{1 + 10^{pH-pK_{a1}}}\right) + [\theta]_{222,mid^2\_pH}\left(1 - \frac{1}{1 + 10^{pH-pK_{a2}}}\right) + [\theta]_{222,(mid^2\_pH-high\_pH)}\left(1 - \frac{1}{1 + 10^{pH-pK_{a3}}}\right)$$

was used for acetylated peptides with the phosphoserine side chain at N1, N2, N3, and helix interior positions. All peptides show the Ser(P) −1 to −2 and Tyr side chain transitions. The Ser(P) N-cap peptide also titrates at its free amine N-terminus.

Peptide concentrations were determined by measuring the tyrosine UV absorbance at 275 nm of diluted aliquots of stock solution in water, using $\epsilon_{275} = 1390\ M^{-1}\ cm^{-1}$. CD measurements are given as mean residual ellipticity at 222 nm ($[\theta]_{222}$) in units of deg cm^2 dmol^{-1}. Helix content was calculated as ($[\theta]_{222}$(observed) − $[\theta]_{222}$(coil))/(−42500(1 − 3/n) − $[\theta]_{222}$(coil)), where $[\theta]_{222}$(coil) is 640 deg cm^2 dmol^{-1} and n is the number of amino acids in the peptide with blocked termini (*29*).

pK_a Calculations. Electrostatics calculations were made with the linearized FDPB method (*30*), using relative dielectric values of 4 for protein/peptide and 78 for water solvent and an ionic strength of 0.01 M (matching to experiment). Graphical analysis was used to establish allowed phosphoserine rotamers at the N-cap, N1, N2, N3, helix center (interior), C3, C2, C1, and C-cap positions in a 15 residue polyalanine α-helix. An acetyl N-terminus and an amide C-terminus were incorporated to match experiment. Calculations were carried out with an uncharged N-terminal amino group. For noncapping locations, the same three phosphoserine rotamers (g^+t, g^-t, tt) at $\chi1$ and $\chi2$ were allowed (with a fixed, staggered configuration at $\chi3$). At the cap positions, two further rotamers were added to these three, based on side chain $\chi3$ angles that were found to be possible with an altered main chain torsion that allows for a closer approach of the phosphoserine side chain to the peptide groups of the helix termini. While this approach was not sufficiently close for extensive hydrogen-bonding, it did provide the opportunity for significant interaction between the phosphate and terminal peptide groups.

At each phosphoserine position the dehydration (also known as the self-energy or Born energy) and peptide solvation (generally known as interaction with the fixed charges or background charges) contributions were calculated for each rotamer (as a difference between values in the peptide and for the single phosphoserine in isolation). The dehydration energy was modified with an empirical term describing the entropy gain associated with liberated water molecules (*31*). Applying this modification lowered ΔpK_a values by about 20% on average (not shown). Overall conclusions derived with and without the modification do not substantially differ. In this linear response model, the electrostatic terms scale with the phosphate charge, so that individual rotamer calculations for charge states −1 and −2 of phosphoserine are derived in parallel. The statistical weights for each rotamer (−1, −2 states) were calculated according to the electrostatic energies, and the electrostatic free energy associated with the phosphate interactions ($G_{es}[P^{1-}]$ or $G_{es}[P^{2-}]$) was obtained from summing the weights. ΔpK_a (relative to isolated phosphoserine) for the −1 to −2 transition was calculated as $\Delta pK_a = (G_{es}[P^{2-}] - G_{es}[P^{1-}])/2.303RT$, R being the universal gas constant and $T = 300$ K. To estimate the relative effects of dehydration and peptide solvation along the helix, this calculation scheme was also used with each of these terms set to zero.

Helix/Coil Theory. Alanine-based peptides in aqueous solution form a complex population of fully helical, fully coil, and partly helical structures. To quantitatively interpret this equilibrium, it is essential to include the structure and stability of every conformation. Lifson−Roig-based helix/coil models do this and now include parameters for helix nucleation, helix interiors, N- and C-capping, and side chain interactions (*12, 29, 32*).

Recently, the theory has been extended to include statistical weights for the N1. N2 and N3 residues with weights defined as n_1, n_2 and n_3, respectively (*21*). An n_1 value is assigned to a helical residue immediately following a coil residue, previously assigned v. The n_1•values and hence helix initiation weight n_1v are low, due to the energetic cost of restricting a residue to a helical conformation without the formation of a hydrogen bond. A helical N2 and a helical N3 residue are assigned weights of n_2w and n_3w, respectively. These new weightings reflect the unique structures adopted by side chains at the N2 and N3 positions, while their previous w weighting associated with hydrogen-bond formation is still maintained. The number of residues with a w weighting is still equal to the number of residues forming main chain−main chain i, $i + 4$ hydrogen bonds. If n_2 and n_3 values for a residue are greater than 1, then this position is preferred over the helix interior. If n_2 and n_3 values are less than 1, the interior is preferred. The use of a helix/coil model with N-cap, N1, N2, and N3 propensities is essential if the results are to be quantified in the form of free energies.

In line with previously determined *n and w* values for the 20 natural amino acids, *n and w* values for phosphoserine were determined using a statistical mechanics algorithm implemented in the program SCINT2 (http://www.bi.umist.ac.uk/users/mjfajdg/scint.htm). SCINT2 implements the modified Lifson−Roig helix/coil theory (*29*) to calculate the helix content of a given peptide sequence. The following are inputs to the program: the peptide sequences and corresponding experimental helix contents; a library of w, v, n_{cap}, and c_{cap} values for each amino acid; an n_{cap} value for acetyl and a c_{cap} value for amide; and a list of parameters to be determined.

n_1, n_2, and n_3 values were determined using the program N1N2N3 (http://www.bi.umist.ac.uk/users/mjfajdg/n1n2n3.htm), which implements the modified Lifson−Roig helix/coil theory of Sun et al. (*21*). The inputs to this program are the peptide sequences; experimental helix contents; a library of w, n_{cap}, n_1, n_2, n_3, c_1 and c_{cap} values for each amino acid; an n_{cap} value for acetyl and a c_{cap} value for amide; and a list of n_1, n_2 and n_3 to be determined. Unknown values were determined in the order n_1, n_2, n_3. When determining n_1 values, n_2, n_3, and c values were set to 1. Similarly when determining n_2 values, n_3 and c values were set to 1. Parameters were varied until they agreed with the experimental helix content.

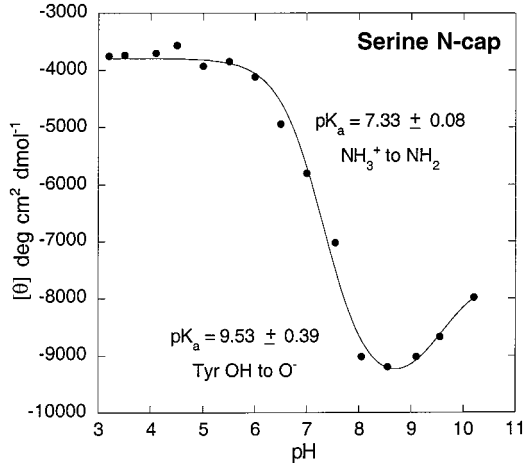

FIGURE 1: pH titration for Ser N-cap peptide.

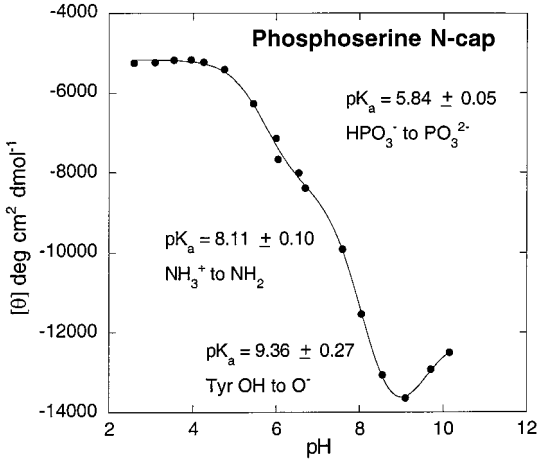

FIGURE 2: pH titration for Ser(P) N-cap peptide.

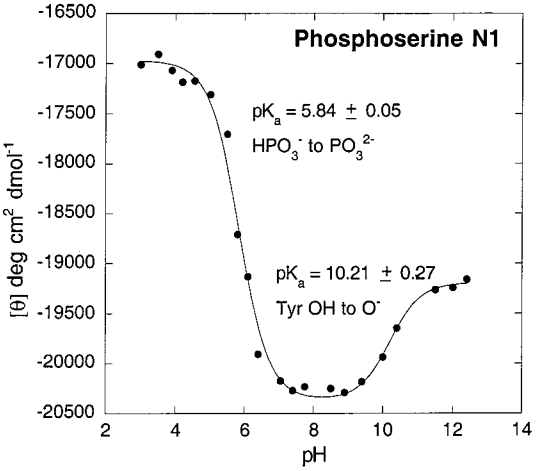

FIGURE 3: pH titration for Ser(P) N1 peptide.

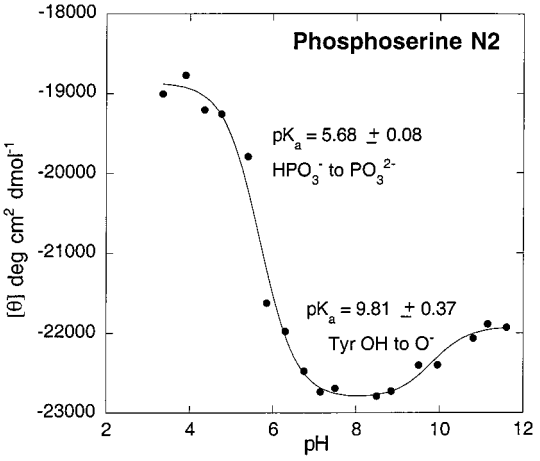

FIGURE 4: pH titration for Ser(P) N2 peptide.

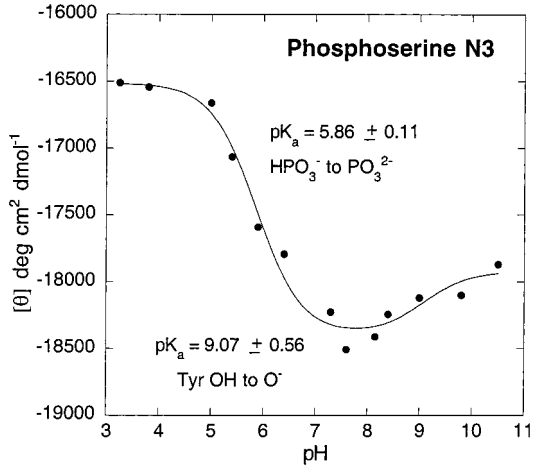

FIGURE 5: pH titration for Ser(P) N3 peptide.

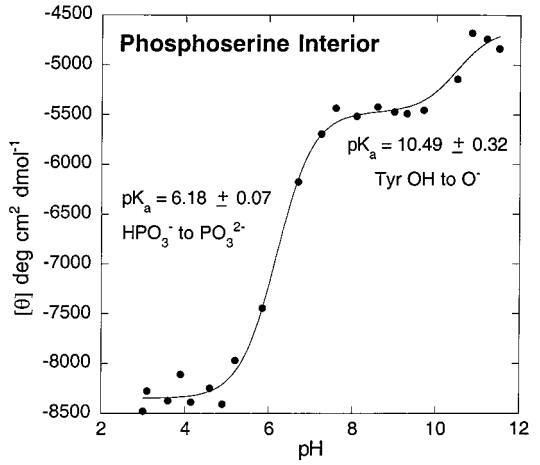

FIGURE 6: pH titration for Ser(P) mid peptide.

RESULTS AND DISCUSSION

Helix Contents of Peptides. Table 1 shows the sequences, mean residual ellipticities, and the helix contents of the synthesized peptides, including values for the singly (−1) and doubly negative (−2) phosphoserine charge states. pH titrations (Figures 1−6) were conducted to determine the pK_a values of the phosphoserine and N-terminus. pH titrations of the Ser N1, Ser N2, Ser N3, and Ser mid peptides were not carried out, as these do not have any titratable groups, apart from the C-terminal Tyr. These measurements are listed in Table 2. The control peptides containing serine at N-cap, N1, N2, and N3 positions have significantly lower helix contents than the peptides that contain double-negative (−2) phosphoserine at the corresponding helix positions. The difference is exceptionally large at N2, where the Ser N2 peptide is 8700 deg cm^2 dmol^{-1} lower than Ser(P) N2 peptide. The average change in ellipticity for the three −1/−2 pairs ($\Delta\theta_{222} = -5650$ deg cm^2 dmol^{-1}) is well outside the range of experimental error (±1000 deg cm^2 dmol^{-1}). These results show qualitatively that a −2 phosphoserine at each

Table 2: pK_a Values in Unacetylated and Phosphoserine Containing Peptides

name	pK_a phosphoserine	pK_a N-terminus
Ser N-cap		7.33
Ser(P) N-cap	5.73	8.11
Ser(P) N1	5.84	
Ser(P) N2	5.69	
Ser(P) N3	5.86	
Ser(P) mid	6.19	

of the four N-terminal positions stabilizes isolated α-helices in water.

The helix contents of the serine control peptides when compared with single negative (−1) phosphoserine peptides at the corresponding helix positions show a notably smaller difference than when compared to the −2 phosphoserine peptides. In the case of Ser(P) N-cap, the −1 state is less helical than the serine control, due to the presence of a positively charged amino N-terminus in the Ser(P) peptide, compared to a neutral amino N-terminus with the serine peptide. It is not possible to measure −1 charged phosphoserine N-cap with a neutral N-terminus, but a correction for the protonation has been estimated when analyzing with helix/coil theory (see below).

In contrast to results at the N-terminus, helix contents decrease for peptides containing phosphoserine residues in the interior compared to serine. Phosphoserine significantly destabilizes peptides when in the interior of the helix, with a −2 phosphoserine having a greater effect than the −1 charge state.

Determination of Helix/Coil Theory Parameters. The experimental CD results were analyzed with the helix/coil models SCINT2 (*29*) and N1N2N3 (*21*), allowing free energies of the interactions to be quantitatively determined. Table 3 shows the experimental helicities of the peptides and their corresponding theoretical helicities as predicted by the algorithms. The five serine control peptide helicities agree well with their theoretical helicities to within experimental error, confirming that the previously measured helix/coil parameters and our helix/coil theory accurately predict the experimental data. The unknown parameters n, n_1, n_2, n_3, and w for phosphoserine and n_3 for serine were determined by adjusting the particular parameter until the calculated helix content was in agreement with experiment. The parameters for both the −1 and −2 phosphoserine states are listed in Table 3. To determine an n value for −1 phosphoserine with a neutral N-terminus, we summed the experimental free energy for a −1 phosphoserine with a positive N-terminus and the mean free energy for protonation of the N-terminus for natural amino acids (0.83 kcal·mol^{-1}) (*13*). It was possible to accurately fit all the experimental helicities except for the doubly charged phosphoserine at N2. An n_2 value for this charge state is too large to currently determine and cannot be assigned in modified helix/coil theory at present. It is likely that a phosphoserine at N2 increases the helix-forming tendencies of residues at N3 and further along the helix, thus propagating its effect. Such effects cannot be taken into account with helix/coil theory, as the n_2 parameter affects only one position in the peptide.

Free Energies. From this fitting we have calculated free energy changes for transfer of −1 or −2 phosphoserine from coil conformation to helical conformation at each of the five positions N-cap, N1, N2, N3, and helix interior (Tables 4−8). These ΔG values are given by $-RT \ln(n)$, $-RT \ln(n_1)$, $-RT \ln(n_2 w)$, $-RT \ln(n_3 w)$, and $-RT \ln(w)$, respectively. Also included is the free energy change relative to alanine ($\Delta\Delta G$ is $\Delta G_{\text{phosphoserine}} - \Delta G_{\text{alanine}}$), the free energy relative to serine ($\Delta\Delta G$ is $\Delta G_{\text{phosphoserine}} - \Delta G_{\text{serine}}$), and the free energy for deprotonation of phosphoserine ($-RT \ln[n_x(-2 \text{ phosphoserine})/n_x(-1 \text{ phosphoserine})]$) at each position. The free energy change for phosphoserine at each helical position relative to serine gives the energy for the direct effect of phosphorylation on serine, similar to phosphorylation in proteins. Table 4 shows estimates of the free energy change for protonation of the phosphoserine N-terminus. Free energies are not available for the −2 state at N2 (Table 6), as we could not determine this n_2 value. The results are summarized in Table 9.

pK_a Values. The pK_a values listed in Table 2 denote the −1 to −2 transition for the phosphoserine side chain at different helical positions. The neutral phosphoserine state and hence −1 to neutral pK_a transition could not be achieved as this would result in the loss of favorable helix macrodipole and capping interactions with the N-terminus and would thus be reached at only very low pH. There was no sign of the onset of this transition for any of our peptides. The measured pK_a values are expected to be lower than the free phosphoserine pK_a values, due to the above-mentioned favorable interactions. In agreement with this theory, the lowest pK_a value for phosphoserine deprotonation is seen at the N2 position. Phosphoserine at this position has the highest helix content, an extremely large n_2, and the highest expected free energy change.

The pK_a value for phosphoserine at an interior position is higher than that at any N-terminal position, due to the destabilizing effect of desolvating the double negative charge at this position. The higher pK_a of the pSer N-terminus compared to Ser is probably due to the loss of favorable electrostatics with the positive N-terminus, even though helix content substantially increases on N-terminus deprotonation· (*13*).

From pH titrations, the helix contents and n values (Tables 1 and 3) of Ser(P) N-cap increase as the phosphoserine becomes more negative and the N-terminus becomes more neutral. A more negative phosphoserine increases its stabilizing interactions with the helix macrodipole plus possible hydrogen bonding with free main chain N−H groups. Although favorable electrostatic interactions between a −1 phosphoserine and a positively charged N-terminus may occur, deprotonation to a neutral N-terminus eliminates repulsive interactions with the helix macrodipole, significantly increasing helix content (*13*).

Analysis of the Ser(P) N-cap helicity with SCINT2 shows that the n value for −2 phosphoserine (Table 3) is the highest known, when compared with the 20 natural amino acid n values (*13*, *29*). A −2 phosphoserine residue at this position is the most preferred N-cap, stabilizing by 1.4 kcal·mol^{-1} relative to Ala, 0.6 kcal·mol^{-1} relative to serine, and 0.3 kcal·mol^{-1} relative to Asp$^-$, the previous most preferred.

The measured n value for −1 phosphoserine with a positive N-terminus is understandably low due the previous helix macrodipole explanation. The corrected value for a neutral N-terminus has an n value (2.25) smaller than that

Table 3: Comparison of Experimental and Theoretical Helicities

name	experimental helicity Ser[a]	theoretical helicity[b]	experimental helicity (P)Ser −1[a]	helix/coil parameters to fit experiment[b]	experimental helicity (P)Ser −2[a]	helix/coil parameters to fit experiment[b]
Ser N-cap	30.5	30.2				
Ser(P) N-cap			23.7[c]	$n = 0.96/2.25$[c]	47.3	$n = 12.15$
Ser N1	49.5	47.5				
Ser(P) N1			50.8	$n_1 = 0.254$	60.6	$n_1 = 2.47$
Ser N2	42.4	42.7				
Ser(P) N2			56.3	$n_2 = 45.90$	67.7	*d*
Ser N3	42.0	*e*		$n_3 = 0.923$		
Ser(P) N3			48.8	$n_3 = 10.66$	54.1	$n_3 = 548$
Ser mid	38.0	42.2				
Ser(P) mid			25.2	$w = 0.125$	17.2	$w = 0.045$

[a] Calculated as $[\theta]_{222}$(observed) − $[\theta]_{222}$(coil)/[−42500(1 − 3/*n*) − $[\theta]_{222}$(coil)], where $[\theta]_{222}$ (coil) is 640 deg cm^2 dmol^{-1} and *n* is the number of amino acids in the peptide, and rounded up to the nearest 100. [b] Ser N-cap and Ser mid predicted helicities and the calculated *n* and *w* values for phosphoserine determined with SCINT2. Ser N1, Ser N2, and Ser N3 predicted helicities and the calculated n_1, n_2, and n_3 values for phosphoserine determined with N1N2N3 program. [c] Corrected *n* value for-1 phosphoserine with neutral N-terminus, using average free energy for protonation of N-terminus (0.83 kcal·mol^{-1}), from Doig and Baldwin (*13*). [d] Not available as unable to fit N2 value for −2 phosphoserine. [e] No prediction, as Ser N3 preference previously unknown

Table 4: Free Energies Values for Phosphoserine at N-cap

	−1 state	−2 state
ΔG[a] of N-capping	−0.4[e]	−1.4
ΔG[b] for protonation of N-terminus	0.5[e]	
$\Delta\Delta G$,[c] relative to serine at N-cap	0.3[e]	−0.6
ΔG[d] for deprotonation of phosphoserine at N-cap (−1 to −2)	−0.9[e]	

[a] $-RT$ ln *n* in kcal·mol^{-1}. [b] $-RT$ ln [*n*(charged N-terminus))/*n*(uncharged N-terminus)] both with −1 phosphoserine, in kcal·mol^{-1}. [c] $\Delta G_{\text{phosphoserine at N-cap}} - \Delta G_{\text{serine at N-cap}}$ in kcal·mol^{-1}. [d] $-RT$ ln[*n*(−2 phosphoserine)/*n*(−1 phosphoserine)] in kcal·mol^{-1}, both with neutral N-terminus. [e] Corrected *n* value for −1 phosphoserine with neutral N-terminus using average free energy for protonation of N-terminus (0.83 kcal·mol^{-1}), from Doig and Baldwin (*13*).

Table 5: Free Energies Values for Phosphoserine at N1

	−1 state	−2 state
ΔG[a] for coil to N1 transition	0.7	−0.5
$\Delta\Delta G$[b] for coil to N1 transition relative to Ala	0.0	−1.2
$\Delta\Delta G$[c] for coil to N1 transition relative to Ser	−0.4	−1.6
ΔG[d] for deprotonation of phosphate (−1 to −2)	−1.2	

[a] $-RT$ ln(n_1) in kcal·mol^{-1}. [b] $\Delta G_{\text{phosphoserine at N1}} - \Delta G_{\text{alanine at N1}}$ in kcal·mol^{-1}, using n_1 alanine value from Cochran et al. (*22*). [c] $\Delta G_{\text{phosphoserine at N1}} - \Delta G_{\text{serine at N1}}$ in kcal·mol^{-1}, using n_1 serine value from Cochran and Doig (*23*). [d] $-RT$ ln [n_1(−2 phosphoserine)/n_1(−1 phosphoserine)] in kcal·mol^{-1}.

Table 6: Free Energies Values for Phosphoserine at N2

	−1 state	−2 state[e]
ΔG[a] relative to helix interior	−2.1	
ΔG[b] for coil to N2 transition	−1.0	
$\Delta\Delta G$[c] for coil to N2 transition relative to Ala	−0.4	
$\Delta\Delta G$,[d] for coil to N2 transition relative to Ser	−1.1	
ΔG[e] for deprotonation of phosphate (−1 to −2)		

[a] $-RT\ln(n_2)$ in kcal·mol^{-1}. [b] $-RT\ln(n_2w)$ in kcal·mol^{-1}. [c] $\Delta G_{\text{phosphoserine }(n_2w)\text{ at N2}} - \Delta G_{\text{alanine }(n_2w)\text{ at N2}}$ in kcal·mol^{-1}. [d] $\Delta G_{\text{phosphoserine }(n_2w)\text{ at N2}} - \Delta G_{\text{serine }(n_2w)\text{ at N2}}$ in kcal·mol^{-1}. [e] Not available as unable to fit N2 value for −2 phosphoserine.

Table 7: Free Energies Values for Phosphoserine at N3

	−1 state	−2 state
ΔG[a] relative to helix interior	−1.3	−3.4
ΔG[b] for coil to N3 transition	−0.2	−1.7
$\Delta\Delta G$[c] for coil to N3 transition relative to Ala		
$\Delta\Delta G$,[d] for coil to N3 transition relative to Ser	−0.7	−2.3
ΔG[e] for deprotonation of phosphate(1 to 2)	−1.6	

[a] $-RT$ ln($n3$) in kcal·mol^{-1}. [b] $-RT$ ln($n3.w$) in kcal·mol^{-1}. [c] Not available as N3 value, for alanine has not been determined. [d] $\Delta G_{\text{phosphoserine }(n_3w)\text{ at N3}} - \Delta G_{\text{serine }(n_3w)\text{ at N3}}$ in kcal·mol^{-1}. [e] $-RT$ ln[n_3w(−2 phosphoserine)/n_3w(−1 phosphoserine)] in kcal·mol^{-1}.

Table 8: Free Energies Values for Phosphoserine at Helix Interior

	−1 state	−2 state
ΔG[a] for coil to helix interior transition	1.1	1.7
$\Delta\Delta G$[b] for coil to helix interior transition relative to Ala	1.4	2.0
$\Delta\Delta G$[c] for coil to helix interior transition relative to Ser	0.6	1.2
ΔG[d] for deprotonation of phosphoserine at interior (−1 to −2)	0.6	

[a] $-RT$ ln *w* in kcal·mol^{-1}. [b] $\Delta G_{\text{phosphoserine }(w)\text{ in helix interior}} - \Delta G_{\text{alanine }(w)\text{ in helix interior}}$ in kcal·mol^{-1}. [c] $\Delta G_{\text{phosphoserine }(w)\text{ in helix interior}} - \Delta G_{\text{serine }(w)\text{ in helix interior}}$ in kcal·mol^{-1}. [d] $-RT$ ln [*w*(−2 phosphoserine)/*w*(−1 phosphoserine)] in kcal·mol^{-1}.

Table 9: Free Energy Changes for Phosphorylating Serine as a Function of Helix Position

	ΔG (kcal·mol^{-1})	
helix position	PO_3H^-	PO_3^{2-}
N-cap	0.3	−0.6
N1	−0.4	−1.6
N2	−1.1	too high to measure
N3	−0.7	−2.3
interior	0.6	1.2

of Ser (3.90) but similar to that of Glu (2.06). This is due to the similar structure, chain length, charge, and hydrogen-bonding capabilities of Glu and −1 phosphoserine at the N-cap. The slightly higher *n* value of the −1 phosphoserine compared to Glu^- could be due to the hydrogen-bonding ability of the serine Oγ plus an added favorable OH group. The preference for a −2 phosphoserine at the N-cap is reflected in the deprotonation of −1 phosphoserine, which stabilizes a helix by −0.9 kcal·mol^{-1}.

In our extended helix/coil theory N1N2N3, residues positioned at N1 in an α-helix have ϕ, ψ dihedral angles restricted to an helical geometry but do not have the benefit of hydrogen-bond formation. Previously measured n_1 values

for the 20 natural amino acids are therefore small compared to n_2 (*22*, *23*) and helix interior positions (w) (*29*). Our results (Tables 3 and 4) show that a −2 phosphoserine has the highest n_1 value at this position and is the only measured residue with a favorable free energy change on transfer from the coil to N1 helical conformation. A −2 phosphoserine at N1 is 1.6 kcal·mol^{-1} more stabilizing than serine, showing the effect of phosphorylating serine at this position. The stabilizing effect is probably favorable electrostatic interactions with the N-terminus.

The singly charged phosphoserine at N1 has a much smaller n_1 value (0.254), between the values of Asp$^-$ (0.284) and Glu$^-$ (0.218), and hence, its positive free energy shows it prefers to be in a coil conformation rather than at a helical N1 position. This is reflected in the deprotonation of −1 phosphoserine, which stabilizes the helix by −1.2 kcal·mol^{-1}.

Phosphoserine has an extremely high preference for the N2 position. This overwhelmingly large n_2 value could be due to the phosphoserine having favorable electrostatic interactions with main chain NH groups in the first two turns of the helix, propagating its stabilizing effect further than our model considers (*33*). The increased availability for hydrogen bonding also favors −2 phosphoserine at this position.

The free energy change for transfer of −1 phosphoserine from coil to helical N2 is 1.0 kcal·mol^{-1}. The n_2 value for −1 phosphoserine is the largest currently determined and preferred over Ala and Ser at the N2 position. Previously the highest at N2 was Glu$^-$ (−1.3 kcal·mol^{-1}). A −1 phosphoserine overwhelmingly prefers to be at N2 by 2.1 kcal·mol^{-1} compared to the interior. Most residues prefer N2 over the interior due to greater side chain conformational freedom and solvent exposure.

Both the −1 and −2 state for phosphoserine have favorable free energy changes at helical N3, relative to the coil position. In agreement with the N-cap, N1, and N2 positions, −2 phosphoserine is preferred to the −1 state at N3. Phosphoserine in either state is highly preferred to serine at this position, showing the favorable effect of serine phosphorylation at N3. This order of preference at N3 is again attributable to electrostatic interactions with the helix macrodipole plus possible hydrogen-bond formation with NH groups. Serine has an n_3 value of 0.92, which means it has little preference for the helix interior over the N3 position. The n_3 values of −1 (11) and −2 (550) phosphoserine reflect their huge preference for N3 relative to the interior, with free energies of 1.3 and 3.4 kcal·mol^{-1}, respectively.

In contrast to the favorable nature of charged phosphoserine at N-terminal positions, a large destabilizing effect is seen with both −2 and −1 phosphoserine at the helix interior (Table 8). The w values of 0.045 and 0.125 for the −2 and −1 states are substantially lower than for alanine (1.70), and positive free energies for the coil to helix interior transition reflect phosphoserine's aversion to the helix interior. An explanation for this observation is that phosphoserine has a large energetic desolvation penalty when positioned within the hydrophobic helix interior. This desolvation effect of the charged phosphate increases as the residue becomes more negative. The solvent accessibility of the bulky phosphoserine is also decreased by regular backbone−backbone $i, i + 4$ hydrogen bonds. This effect is unseen at the N-terminus due to favorable electrostatics, main chain−side chain hydrogen bonding, and better solvent accessibility.

Structural Studies. We have identified protein crystal structures that contain phosphorylated serine residues in α-helices. Although only eight structures are available, each one contains the phosphoserine residue at the N-terminus of the helix, in line with its preference for the N-terminal position in our experimental results. Although structures with phosphoserine in the helix interior are not available, phosphorylation of serine at these sites in proteins may well affect function by destabilizing and disrupting helical and surrounding structure.

Three structures (4ICD, 1APM, and 1FUO) contain phosphoserine at the N-cap position. Phosphorylation at the α-helix N-cap occurs in the histidine containing protein (HPr) of the phosphoenol-pyruvate:sugar-phosphotransferase system from *Bacillus subtilis* (1FUO). When phosphorylated at Ser46, increased helix stabilization results without conformational change through helix macrodipole interactions, as it may be too bulky to hydrogen bond (*24*). Phosphoserine adopts the trans $\chi 1$ rotamer and maintains the Oγ to N3 NH hydrogen bond, similar to serine. This phosphoserine at the N-cap may possibly H-bond to the same N3 NH with one of its phosphate oxygens. Similarly, the phosphorylated Ser113 N-cap of Isocitrate dehydrogenase (4ICD) is again trans and points toward the helix, possibly hydrogen bonding to the N3 NH. The phosphorylated Ser10 N-cap of cAMP-dependent protein kinase (1APM) points away from the helix without any possibility of hydrogen bonding. The cAMP-dependent protein kinase could contain a singly charged phosphoserine behaving like Glu$^-$, which is a bad N-cap. The Glu$^-$ side chain is too long to hydrogen bond to NH groups, so it adopts the gauche$^+$ rotamer and points away from the helix. Previous studies show side chain hydrogen bonding is the main stabilizing factor at the N-cap due to their linear geometry (*13*, *17*). The hydrogen-bonding capability of phosphoserine plus electrostatic interactions with the helix macrodipole accounts for its high preference at the N-cap.

There are three structures with phosphoserine at N2. The phosphate group of Ser133 at N2 of KID in the KID−KIX complex of 1KDX adopts the uncommon g$^-$, g$^+$ rotamer and hydrogen bonds to its own NH group as well as forming salt bridges to the Arg N-cap. This phosphoserine also forms favorable electrostatics with helical residues Tyr568 and Lys662 of the KIX domain (*34*). These phosphoserine capping interactions at N2 are similar to those of Glu, which also regularly forms the same rare interior helical g$^-$, g$^+$ rotamer conformation at N2, hydrogen bonding to itself (*18*). Both Glu and phosphoserine residues when at N2 potentially compete with good N-caps such as Asp and Asn for the N2 NH group. Similar to the observed phosphoserine KID structure, Asp at N2 when g$^-$ always forms the i, i main chain−side chain hydrogen bond and regularly forms salt bridges to Arg at the N-cap. This Arg-X-(P)Ser hydrogen-bonding network for phosphoserine at N2 could be a good predictor and possible initiator for a helix, more so than Arg-X-Asp. Although Ser58 at the N2 helix position within 1AUZ is phosphorylated in bacterial regulatory pathways, only NMR structures of the unphosphorylated form are available. 1OVA is phosphorylated at Ser87, the N2 position in a stretch of α and 3_{10} helix, but the g$^+$ $\chi 1$ rotamer is adopted

and hydrogen-bond formation does not occur.

Although our peptides are designed to avoid side chain interactions with the N-cap (acetyl has no side chain), these are possible in proteins with phosphoserine at N2. If a good N-cap is not present, phosphoserine may form an *i*, *i* + 1 side chain−main chain hydrogen bond to the N3 NH group, similar to that of Glu and Asp. These *i*, *i* and *i*, *i* + 1 hydrogen bonds to NH groups that are possible in our peptides, coupled with helix macrodipole interactions, give weight to our large value for n_2.

Previous measurements at N2 and N1 show that negatively charged residues such as Asp and Glu are preferred, but not hydrogen-bonding residues such as Asn, Ser, and Thr, which are good N-caps (*22*, *23*). The bad nonlinear geometry of side chain hydrogen bonds with NH groups when a residue is at N2 or N1 compared to the N-cap suggests that electrostatic interactions with the macrodipole have the greater stabilizing effect for phosphoserine at these two positions.

Two structures are available with phosphoserine at N1, 1HJK, and 1OVA. These have phosphoserine-102 and phosphoserine-350, both in the $\chi 1$ g^+ rotamer, pointing away from the helix N-terminus without hydrogen-bond formation. Crystal structure data (*18*) has revealed that residues such as Asp, Glu, and Gln have lower preferences at N1 than N2, due to N1 being less solvent exposed. Hydrophobic residues have higher preferences at N1 than at other N-terminal positions. Glu due to its chain length cannot form favorable hydrogen bonds when at N1. These observations and our experimental evidence show that phosphoserine will not have as large an effect at N1 compared to N2. Although it will form favorable electrostatics with the helix macrodipole, any hydrogen-bond formation that is possible is dependent on the N2 residue, which if highly preferred at N2 will usually win over an N1 phosphoserine in competition for NH bonding partners. The N1 side chain to N1 NH hydrogen bond will not be affected by the N2 residue and is always available to phosphoserine at N1.

A simulation with phosphoserine at the N1 position in an acetylated alanine peptide was shown to stabilize the helix through electrostatic interactions between the phosphate and helix backbone (*25*). Hydrogen bonds were not observed between the phosphate and free NH groups.

Although there are no structures present, the preference for the g^- rotamer for phosphoserine at N3 is expected to be lower compared to N2. This is due to steric clashes with the N-cap CO group. Hydrogen bonding with the N4 NH is not possible, as this is involved in main chain *i*, *i* + 4 bonds. The *i*, *i* side chain−main chain hydrogen bond is also less preferred at N3. A phosphoserine at N3 may well form a capping box in proteins (*35*, *36*), hydrogen bonding to the N-cap NH, while the N-cap side chain hydrogen bonds to the N3 NH. Glu regularly adopts this motif when in the gauche$^+$ rotamer. This is not possible in our peptides, due to the lack of an NH in the acetyl N-cap.

Our sequences were specifically designed to avoid side chain interactions, but in nature, phosphoserine could potentially have a number of side chain−side chain interactions when placed at the N-terminus, such as salt bridges to Lys and Arg plus hydrogen bonds to Asn.

Phosphoserine has an extremely low *w* value and is not stabilizing when placed in the helix interior, due to the large penalty for desolvating the bulky side chain phosphate group. Our results agree well with those measured previously for phosphoserine in the helix interior of a coiled coil leucine zipper. Phosphorylation of a serine residue that is not involved in hydrophobic contact with the other helix and projecting into solvent destabilizes the protein by 1 kcal·mol^{-1} per residue (*26*), due to a desolvation effect. When Ser is placed in a similar structure closer to the hydrophobic interface and neighboring Arg residues, the protein is stabilized by 0.7 kcal·mol^{-1}, due to a network of inter and intrahelical interactions (*37*).

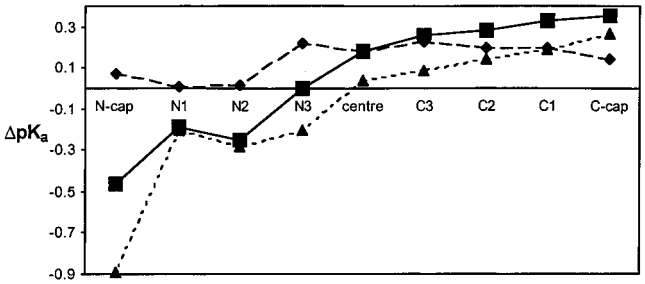

FIGURE 7: Calculated ΔpK_a values as a function of helix position, showing dehydration (diamond), protein solvation (triangle) and total effects (square).

pK_a Calculations: The Balance of Peptide Solvation and Dehydration. To further rationalize our empirical results and protein structure survey, we performed free energy calculations on phosphorylation effects in helices. The most convenient reference point between experiment and theory is the −1 to −2 phosphoserine pK_a, since experimentally this is a direct measurement associated with a structural transition and since calculated ΔpK_a values relate to interactions in the helical peptide. Comparison of pH-dependent free energies would be more complicated, since models for the denatured states would be required (*38*). Figure 7 shows calculated ΔpK_a values along the helix, relative to an isolated phosphoserine. Considering the pK_a changes from the N1, N2, and N3 sites, where the experimental data do not require correction for a positive amino group, to the helix center, the calculated ranges (0.35, 0.50, 0.33) are in reasonable agreement with theory (0.37, 0.43, 0.18). Theory and experiment both give a moderately enhanced stabilization at the N2 site relative to N1 and N3.

Positive values in Figure 7 denote stabilization and negative values destabilization. On this basis, theory predicts a transition from stabilizing to destabilizing at N3, whereas experiment shows that phosphoserine at N3 is stabilizing, so that there is some discrepancy in the detail of this transition point. However, the general agreement allows us to use the notional dehydration and peptide solvation ΔpK_a contributions shown in Figure 7 to have informed discussion of the molecular origins underlying the measurements. At the helix center the dehydration term dominates a relatively small peptide solvation contribution, giving the destabilization suggested by Szilak et al. (*26*). Toward the N-terminus, the desolvation term decreases as the helix bulk is reduced, allied to increasingly favorable interactions with the peptide NH groups, leading to the overall stabilization. At the N-cap position the additional rotamers that are possible with terminal main chain torsion, allow more favorable peptide solvation of phosphoserine, along with a slight increase in the dehydration penalty from approach of the phosphate

group to the helix terminus.

Interestingly, the theoretical curve permits investigation of the C-terminal region, in which the destabilizing regime mitigates against peptide experiments due to lack of helical content. While the dehydration term decreases somewhat from its central peak, this decline is more than offset by increasingly unfavorable peptide solvation, with the net result that C-cap, C1, C2, and C3 locations are more destabilizing than the central helix position. The calculated sharp change in peptide solvation from N1 to N-cap is not mirrored from C1 to C-cap, since the equivalent interactions are unfavorable and are weighted down statistically.

CONCLUSION

Our study shows that positioning phosphoserine at the N-terminus stabilizes a helix, through electrostatic interactions with the helix dipole. When positioned at the helix interior, phosphoserine destabilizes due to a desolvation penalty associated with the phosphate group. When the phosphoserine side chain is in its −1 state, it behaves very similarly to Glu, both in terms of energetics and structure. This is logical, since the side chains are then almost isosteric, with the same number of bonds from the backbone to the negative charged oxygens. When phosphoserine has a −2 charge, it forms very strong interactions, making it more favorable at N-cap, N1, N2, and N3 than any other amino acid. This may shed light on the general mechanism of phosphorylation on protein structure. Phosphorylation at the N-terminus has a powerful stabilizing effect on helices, as previously suggested for the HPr protein by Pullen et al. Similarly, phosphorylation at the helix interior or C-terminal positions may destroy helical structure. Electrostatic interactions involving −2 phosphoserine are stronger than any interaction involving the standard 20 amino acids and can thus readily alter protein structure. Alternatively, the addition of a phosphate group may affect protein function sterically, by simply blocking access to a binding site, for example.

ACKNOWLEDGMENT

We thank Ian Fleet and Simon Gaskell at the Simon Barber Centre for Mass Spectrometry, UMIST, for peptide verification and Duncan Cochran for useful discussions.

REFERENCES

1. Marks, F. (1996) *Protein Phosphorylatyion*, VCH Verlagsgesellachaft, Weinheim, Germany.
2. Chou, P. Y., and Fasman, G. D. (1974) *Biochemistry 13*, 211−22.
3. Levitt, M. (1978) *Biochemistry 17*, 4277−85.
4. Williams, R. W., Chang, A., Juretic, D., and Loughran, S. (1987) *Biochim. Biophys. Acta 916*, 200−4.
5. Argos, P., and Palau, J. (1982) *Int. J. Pept. Protein Res. 19*, 380−93.
6. Richardson, J. S., and Richardson, D. C. (1988) *Science 240*, 1648−52.
7. Kumar, S., and Bansal, M. (1998) *Proteins 31*, 460−76.
8. Yumoto, N., Murase, S., Hattori, T., Yamamoto, H., Tatsu, Y., and Yoshikawa, S. (1993) *Biochem. Biophys. Res. Commun. 196*, 1490−1495.
9. Chakrabartty, A., Doig, A. J., and Baldwin, R. L. (1993) *Proc. Nat. Acad. Sci. U.S.A. 90*, 11332−6.
10. Forood, B., Feliciano, E. J., and Nambiar, K. P. (1993) *Proc. Nat. Acad. Sci. U.S.A. 90*, 838−42.
11. Lyu, P. C., Wemmer, D. E., Zhou, H. X., Pinker, R. J., and Kallenbach, N. R. (1993) *Biochemistry 32*, 421−5.
12. Doig, A. J., Chakrabartty, A., Klingler, T. M., and Baldwin, R. L. (1994) *Biochemistry 33*, 3396−403.
13. Doig, A. J., and Baldwin, R. L. (1995) *Protein Sci. 4*, 1325−36.
14. Serrano, L., Sancho, J., Hirshberg, M., and Fersht, A. R. (1992) *J. Mol. Biol. 227*, 544−59.
15. Lecomte, J. T. J., and Moore, C. D. (1991) *J. Am. Chem. Soc. 113*, 9663−9665.
16. Bell, J. A., Becktel, W. J., Sauer, U., Baase, W. A., and Matthews, B. W. (1992) *Biochemistry 31*, 3590−6.
17. Doig, A. J., MacArthur, M. W., Stapley, B. J., and Thornton, J. M. (1997) *Protein Sci. 6*, 147−55.
18. Penel, S., Hughes, E., and Doig, A. J. (1999) *J. Mol. Biol. 287*, 127−43.
19. Petukhov, M., Munoz, V., Yumoto, N., Yoshikawa, S., and Serrano, L. (1998) *J. Mol. Biol. 278*, 279−89.
20. Petukhov, M., Uegaki, K., Yumoto, N., Yoshikawa, S., and Serrano, L. (1999) *Protein Sci. 8*, 2144−50.
21. Sun, J. K., Penel, S., and Doig, A. J. (2000) *Protein Sci. 9*, 750−4.
22. Cochran, D. A. E., Penel, S., and Doig, A. J. (2001) *Protein Sci. 10*, 463−470.
23. Cochran, D. A. E., and Doig, A. J. (2001) *Prot. Sci. 10*, 1305−1311.
24. Pullen, K., Rajagopal, P., Branchini, B. R., Huffine, M. E., Reizer, J., Saier, M. H. J., Scholtz, J. M., and Klevit, R. E. (1995) *Protein Sci. 4*, 2478−86.
25. Smart, J. L., and McCammon, J. A. (1999) *Biopolymers 49*, 225−33.
26. Szilak, L., Moitra, J., Krylov, D., and Vinson, C. (1997) *Nat. Struct. Biol.4*, 112−4.
27. Padmanabhan, S., Marqusee, S., Ridgeway, T., Laue, T. M., and Baldwin, R. L. (1990) *Nature 344*, 268−70.
28. Chakrabartty, A., Kortemme, T., Padmanabhan, S., and Baldwin, R. L. (1993) *Biochemistry 32*, 5560−5565.
29. Rohl, C. A., Chakrabartty, A., and Baldwin, R. L. (1996) *Prot. Sci. 5*, 2623−2637.
30. Warwicker, J. (1998) *J. Biol. Chem. 273*, 2501−4.
31. Warwicker, J. (1997) *Protein Eng. 10*, 809−14.
32. Stapley, B. J., Rohl, C. A., and Doig, A. J. (1995) *Prot. Sci. 4*, 2383−91.
33. Tidor, B. (1994) *Proteins 19*, 310−23.
34. Mestas, S. P., and Lumb, K. J. (1999) *Nat. Struct. Biol.6*, 613−4.
35. Dasgupta, S., and Bell, J. A. (1993) *Int. J. Pept. Protein Res. 41*, 499−511.
36. Harper, E. T., and Rose, G. D. (1993) *Biochemistry 32*, 7605−9.
37. Szilak, L., Moitra, J., and Vinson, C. (1997) *Protein Sci. 6*, 1273−83.
38. Warwicker, J. (1999) *Protein Sci. 8*, 418−25.

BI0113216